Cell Reports, Volume *32*

Supplemental Information

Cycling Stem Cells Are Radioresistant and Regenerate the Intestine

Xiaole Sheng, Ziguang Lin, Cong Lv, Chunlei Shao, Xueyun Bi, Min Deng, Jiuzhi Xu, Christian F. Guerrero-Juarez, Mengzhen Li, Xi Wu, Ran Zhao, Xu Yang, Guilin Li, Xiaowei Liu, Qingyu Wang, Qing Nie, Wei Cui, Shan Gao, Hongquan Zhang, Zhihua Liu, Yingzi Cong, Maksim V. Plikus, Christopher J. Lengner, Bogi Andersen, Fazheng Ren, and Zhengquan Yu

Figure S1 (Related to Figure 1)

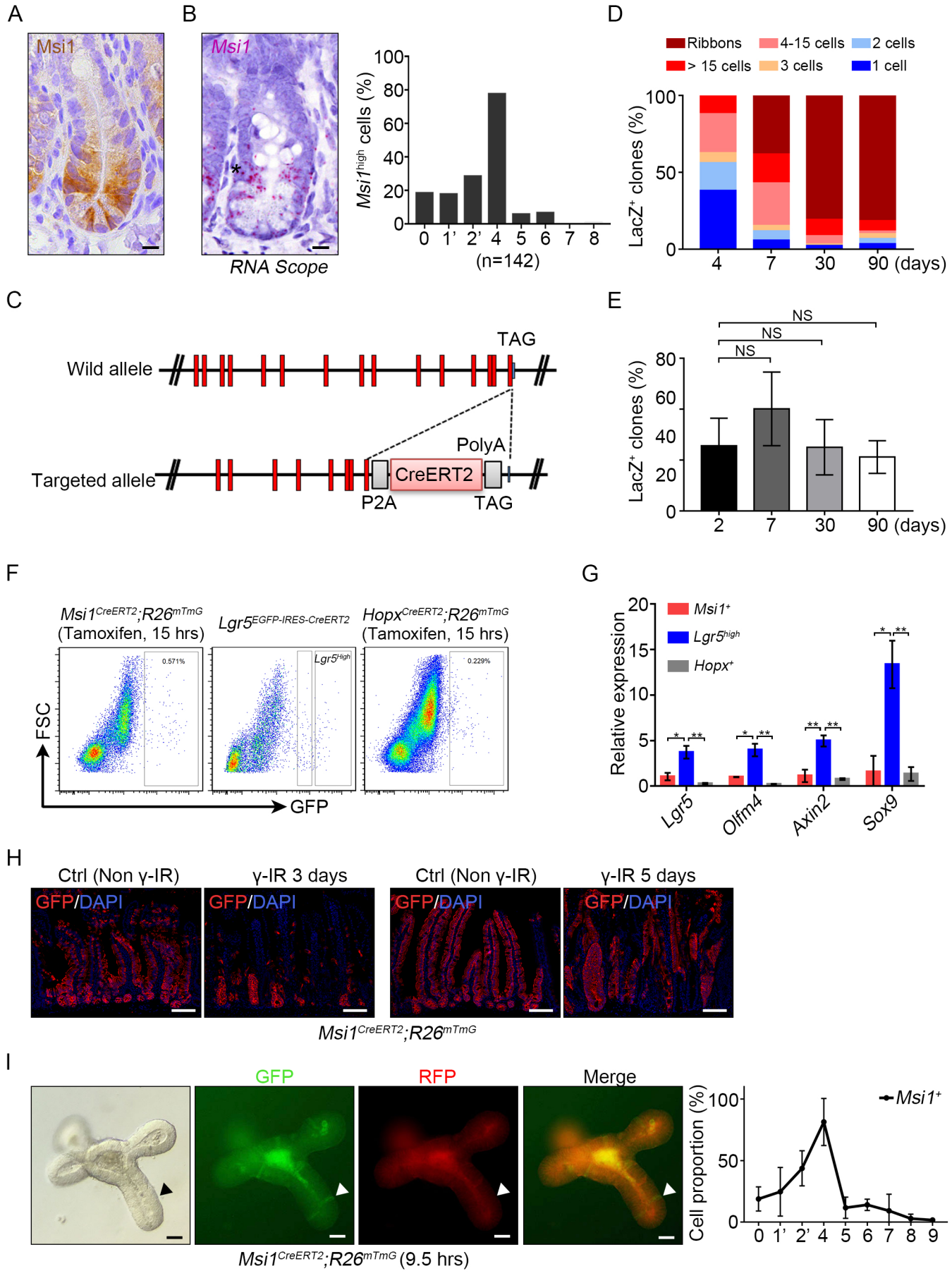

Figure S1. Generation of *Msi1*^{CreERT2} knockin mouse. Related to Figure 1.

(A) Immunohistochemistry for Msi1 in mouse intestinal crypts. n = 3 mice. Scale bar: 10 μm. (B) *In situ* hybridization for *Msi1* in mouse intestines with RNAscope methods (left). * indicates cells highly expressing *Msi1* mRNA (*Msi1*^{high}). Scale bar: 10 μm. Quantification of *Msi1*^{high} cells at indicated position (Right). n = 142 crypts. (C) Schematic representation of the *Msi1*^{CreERT2} targeting vector. (D) Quantification of LacZ^{+} clone size in intestinal crypts of *Msi1*^{CreERT2}*;R26R*^{LacZ} mice at the indicated chase time. n=195 images analyzed, 270-663 crypts and 3 mice per chase timepoint were analyzed. (E) LacZ^{+} clone frequency in intestinal crypts of *Msi1*^{CreERT2}*;R26R*^{LacZ} mice at the indicated chase timepoint. n = 195 images analyzed, 270-663 crypts and 3 mice per chase timepoint were analyzed. Data represent the mean value ± SD. NS, not significant (Student's t-test). (F) Flow cytometry analysis of intestinal epithelial cells from *Lgr5*$^{EGFP\text{-}CreERT2}$ mice, and in sorted *Msi1*$^{+}$ and *Hopx*$^{+}$ cells in *Msi1*^{CreERT2}*;R26*^{mTmG} and *Hopx*^{CreERT2}*;R26*^{mTmG} mice fifteen hours after TAM induction. (G) qRT-PCR analysis for *Lgr5*, *Olfm4*, *Axin2* and *Sox9* in sorted *Lgr5*^{high} cells from *Lgr5*$^{EGFP\text{-}IRES\text{-}CreERT2}$ mice and in sorted *Msi1*$^{+}$ and *Hopx*$^{+}$ cells in *Msi1*^{CreERT2}*;R26*^{mTmG} and *Hopx*^{CreERT2}*;R26*^{mTmG} mice fifteen hours after tamoxifen induction, as shown in Panel F. n = 3 mice. Data represent the mean value ± SD. *P<0.05; **P<0.01 (Student's t-test). Two-way ANOVA analysis was performed. The p value between *Msi1*$^{+}$ and *Lgr5*$^{+}$ cells is less than 0.0001, while the p value between *Msi1*$^{+}$ and *Hopx*$^{+}$ cells is 0.3618. (H) Representative images of GFP^{+} ribbons in *Msi1*^{CreERT2}*;R26*^{mTmG} lineage-labeled small intestines four and six days after TAM induction, or the mice were irradiated after fifteen-hour TAM exposure, and harvested three and five days after γ-IR. n=3 mice per chase timepoint. Scale bar: 50 μm. (I) Immunofluorescence for GFP in organoids from *Msi1*^{CreERT2}*;R26R*^{mTmG} mice 9.5 hours after 4-OH induction (n=115 Crypts, n=4 mice). Quantification of the proportion of GFP^{+} cells at indicated position. Data represent the mean value ± SD. Scale bar: 50 μm.

Figure S2 (Related to Figure 1)

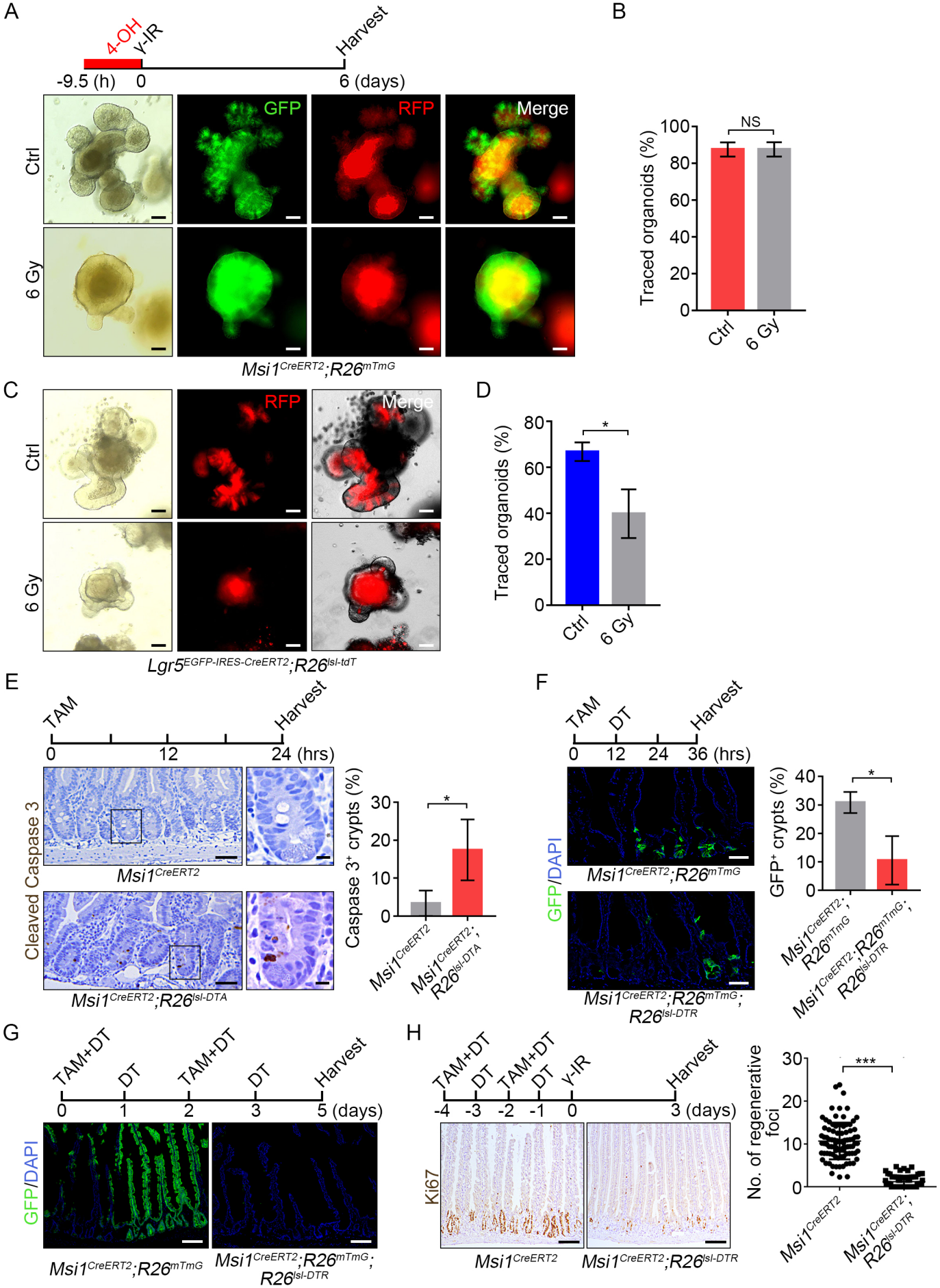

Figure S2: *Msi1*$^{+}$ cells are more DNA damage-resistant than *Lgr5*^{high} cells. Related to Figure 1.

(A) Representative images of organoids in *Msi1*^{CreERT2}*;R26R*^{mTmG} lineage-labeled small intestines. Control, *Msi1*^{CreERT2}*;R26R*^{mTmG} mice were traced for 6 days after 4-OH induction (n=95 Crypts, n=3 mice); 6 Gy, the mice were irradiated with a dose of 6 Gy after 9.5 hours of 4-OH exposure, and then traced for 6 days (n=85 Crypts, n=3 mice). Scale bar: 50 μm. (B) Quantification of GFP^{+} organoids under the indicated conditions in Panel A. Data represent the mean value ± SD. NS, not significant (Student's t-test). (C) Representative images of GFP^{+} organoids in *Lgr5*$^{EGFP\text{-}IRES\text{-}CreERT2}$*;R26*$^{lsl\text{-}tdT}$ lineage-labeled small intestines. Control, *Lgr5*$^{EGFP\text{-}IRES\text{-}CreERT2}$*;R26*$^{lsl\text{-}tdT}$ mice were traced for 6 days after 4-OH induction (n=99 Crypts, n=3 mice); 6 Gy, the mice were irradiated with a dose of 6 Gy after 9.5 hours of 4-OH exposure, and then traced for 6 days (n=134 Crypts, n=3 mice). Scale bar: 50 μm. (D) Quantification of GFP^{+} organoids under the indicated conditions in Panel C. Data represent the mean value ± SD. **P*<0.05 (Student's t-test). (E) Immunohistochemistry for cleaved caspase 3 in *Msi1*^{CreERT2} (n=166 crypts, n=3 mice) and *Msi1*^{CreERT2}*;R26*$^{lsl\text{-}DTA}$ (n=228 crypts, n=3 mice) mice 24 hours after TAM induction. Scale bar: 50 μm (left), 10 μm (right). Quantification of cleaved caspase 3^{+} crypts. Data represent the mean value ± SD. **P*<0.05 (Student's t-test). (F) Immunofluorescence for GFP in intestinal crypts and quantification of GFP^{+} crypts from *Msi1*^{CreERT2}*;R26*^{mTmG} (n=117 crypts, n=3 mice) and *Msi1*^{CreERT2}*;R26*$^{mTmG;}$R26$^{lsl\text{-}DTR}$ (n=116 crypts, n=3 mice) mice at indicated conditions. Scale bar: 50 μm. Data represent the mean value ± SD. **P*<0.05 (Student's t-test). (G) Shematic showing the strategy of deleting *Msi1*$^{+}$ cells. Immunofluorescence for GFP in *Msi1*^{CreERT2}*;R26*^{mTmG} and *Msi1*^{CreERT2}*;R26*$^{mTmG;}$R26$^{lsl\text{-}DTR}$ mice after four consecutive DT induction. Scale bar: 100 μm. (H) Immunohistochemistry for Ki67 in *Msi1*^{CreERT2} and *Msi1*^{CreERT2}*;R26*$^{lsl\text{-}DTR}$ mice under the indicated conditions. The mice were irradiated one day after the last DT induction, and then the samples were harvested three days after γ-IR. Scale bar: 100 μm. Quantification of regenerative foci (Ctrl, n=92 images analyzed, n=3 mice; DTR, n=73 images analyzed, n=3 mice). Data represent the mean value ± SD. ****P*<0.001 (Student's t-test).

Figure S3 (Related to Figure 2)

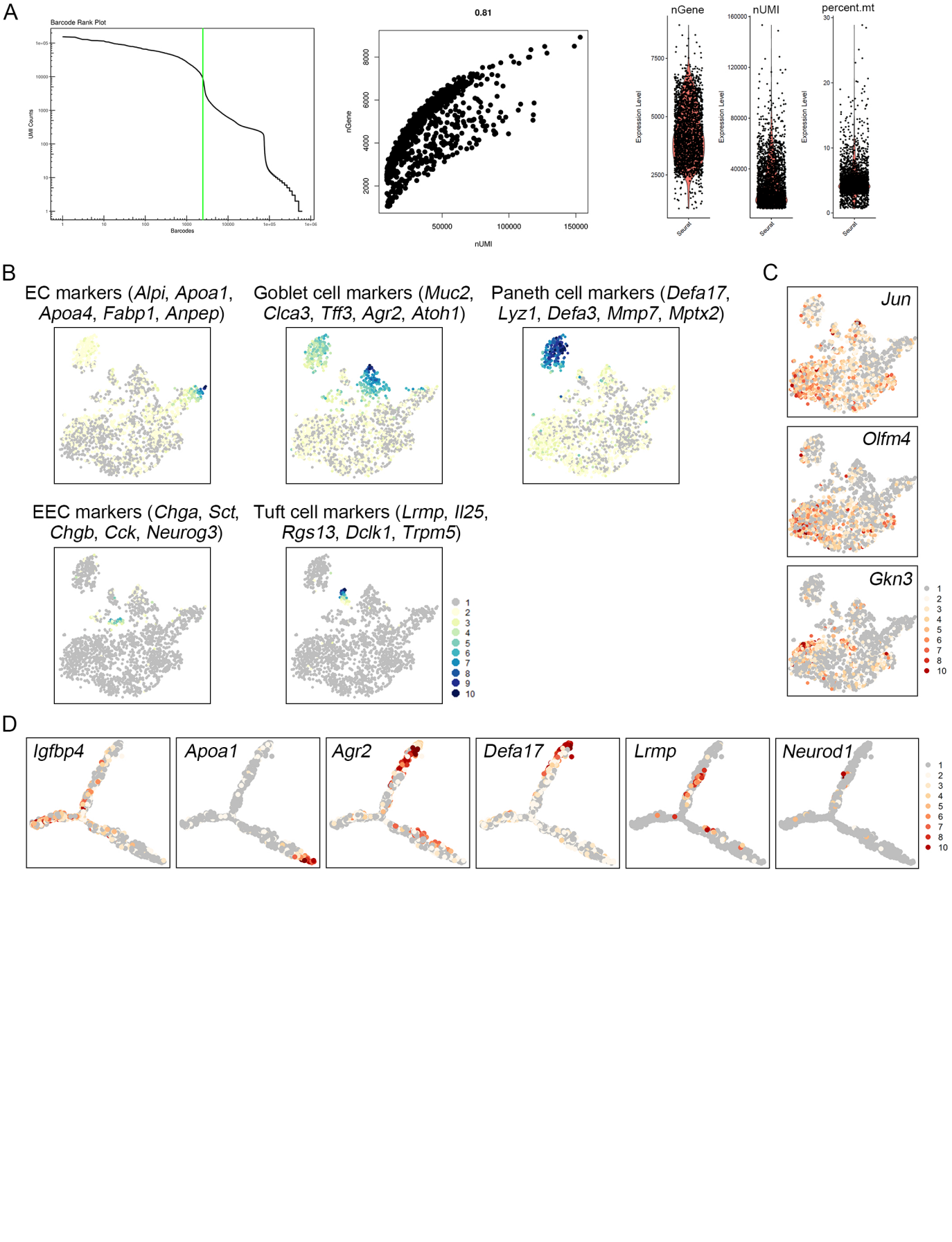

Figure S3. Quality control metrics of scRNA-seq analysis from *Msi1*$^{+}$ cells. Related to Figure 2.
(A) scRNA-seq data quality control of *Msi1*$^{+}$ cells sorted from *Msi1*^{CreERT2}*;R26*^{mTmG} mice fifteen hours after TAM induction. Uniqe molecular identifiers (UMIs): 28753 UMIs per cell, 4316 genes per cells. The number of UMIs, genes, and mitochondrial percentage contents detected per cell. The green line mark cutoffs for selecting cells. (B) Mean expression ($\log_2$(TMP+1)) of several marker genes for a particular cell type shown on t-SNE plots. (C) Feature plots of expression distribution for ISC marker genes, *Jun*, *Olfm4* and *Gkn3*. Expression levels for each cell are color-coded. (D) Expression levels of the ISC marker *Igfbp4*, the EC marker *Apoa1*, the goblet cell marker *Agr2*, the Paneth cell marker *Defa17*, the tuft cell marker *Lrmp* and the EEC marker *Neurod1* shown as a pseudotime feature plot. Expression levels for each cell are color-coded.

Figure S4 (Related to Figure 3)

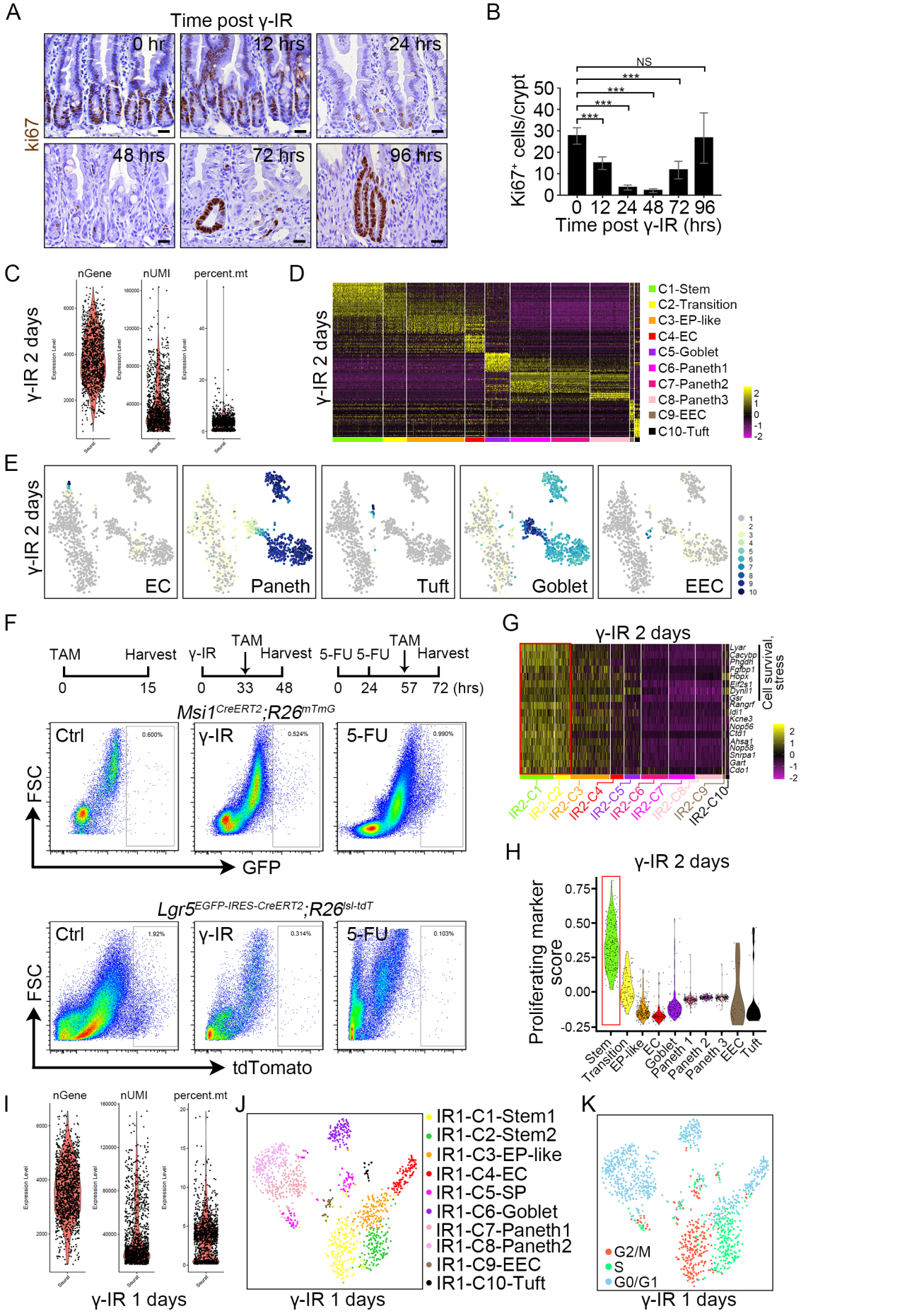

Figure S4. Cycling ISCs initiate intestinal epithelial regeneration. Related to Figure 3.

(A) Immunohistochemistry for Ki67 in the intestine at the indicated time points after γ-IR. Scale bar: 20 μm. (B) Quantification of $Ki67^+$ cells per crypt in Panel A (n=254 crypts, n=3 mice per chase timepoint). Data represent the mean value ± SD. NS, not significant; ***P<0.001 (Student's t-test). (C) scRNA-seq data quality control of $Msi1^+$ cell progeny from $Msi1^{CreERT2};R26^{mTmG}$ mice two days after γ-IR. The mice were pretreated with TAM fifteen hours before irradiation. The number of UMIs, genes, and mitochondrial percentage contents detected per cell. (D) Heatmap of differentially expressed genes in each cluster two days after γ-IR. (E) Mean expression ($\log_2$(TMP+1)) of several marker genes for a particular cell type shown on t-SNE plots, the selected marker genes were identical to Figure S3B. (F) $Msi1^+$ cells are more radioresistant to DNA damage stress than $Lgr5^+$ cells. Mice were treated with γ-IR or two consecutive doses of 5-FU and then induced by TAM fifteen hours before sacrifice. The quantification results were shown in Figure 3D. (G) Heatmap of cell survival genes in distinct clusters two days after γ-IR. (H) Violin plots of proliferating marker score in distinct clusters two days after γ-IR. (I) scRNA-seq data quality control of $Msi1^+$ cell progeny from $Msi1^{CreERT2};R26^{mTmG}$ mice one day after γ-IR. The mice were pretreated with tamoxifen fifteen hours before irradiation. The number of UMIs, genes, and mitochondrial percentage contents detected per cell. (J) A t-SNE plot revealed cellular heterogeneity with ten distinct clusters of 1271 $Msi1^+$ cell progeny from $Msi1^{CreERT2};R26^{mTmG}$ mice one day after γ-IR. The mice were pretreated with TAM fifteen hours before irradiation. General identity of each cell cluster is defined on the right. (K) Cell cycle metrics on $Msi1^+$ cell progeny one day after γ-IR. t-SNE plot of assigned cycling stages on $Msi1^+$ cell progeny. Cells in S phase are colored green, those in G2/M phase are red, and those in G0/G1 phase are blue.

Figure S5 (Related to Figure 4)

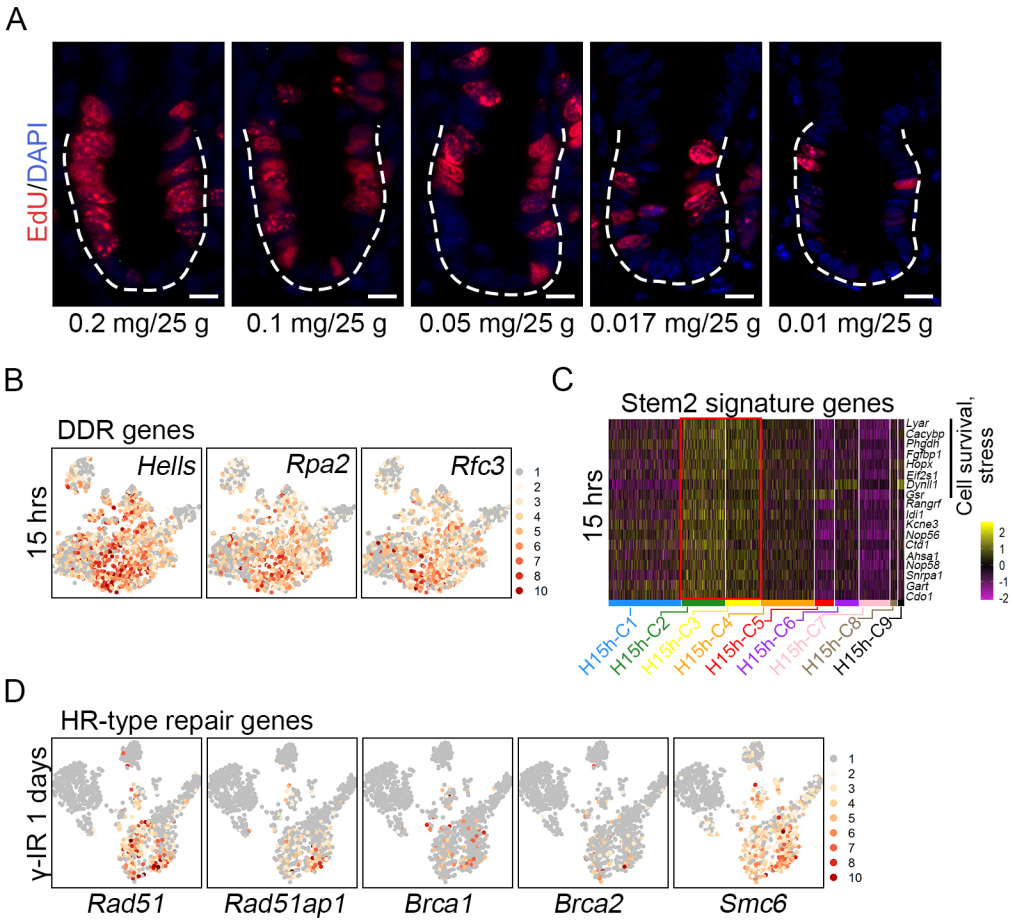

Figure S5. *Msi1*$^{+}$ cells are more rapidly cycling compared to CBCs. Related to Figure 4.

(A) Immunofluoresence for EdU in intestinal crypts after a 90 min pulse of EdU at the indicated concentration. Scale bar, 10 μm. (B) Feature plots of expression distribution for DDR genes in *Msi1*$^{+}$ cells at homeostasis. Expression levels for each cell are color-coded. (C) Heatmap of genes functioning on cell survival and stress in distinct clusters. (D) Feature plots of expression distribution for the key genes functioning in HR-type DNA damage repair one day after irradiation. Expression levels for each cell are color-coded.

Figure S6 (Related to Figure 5)

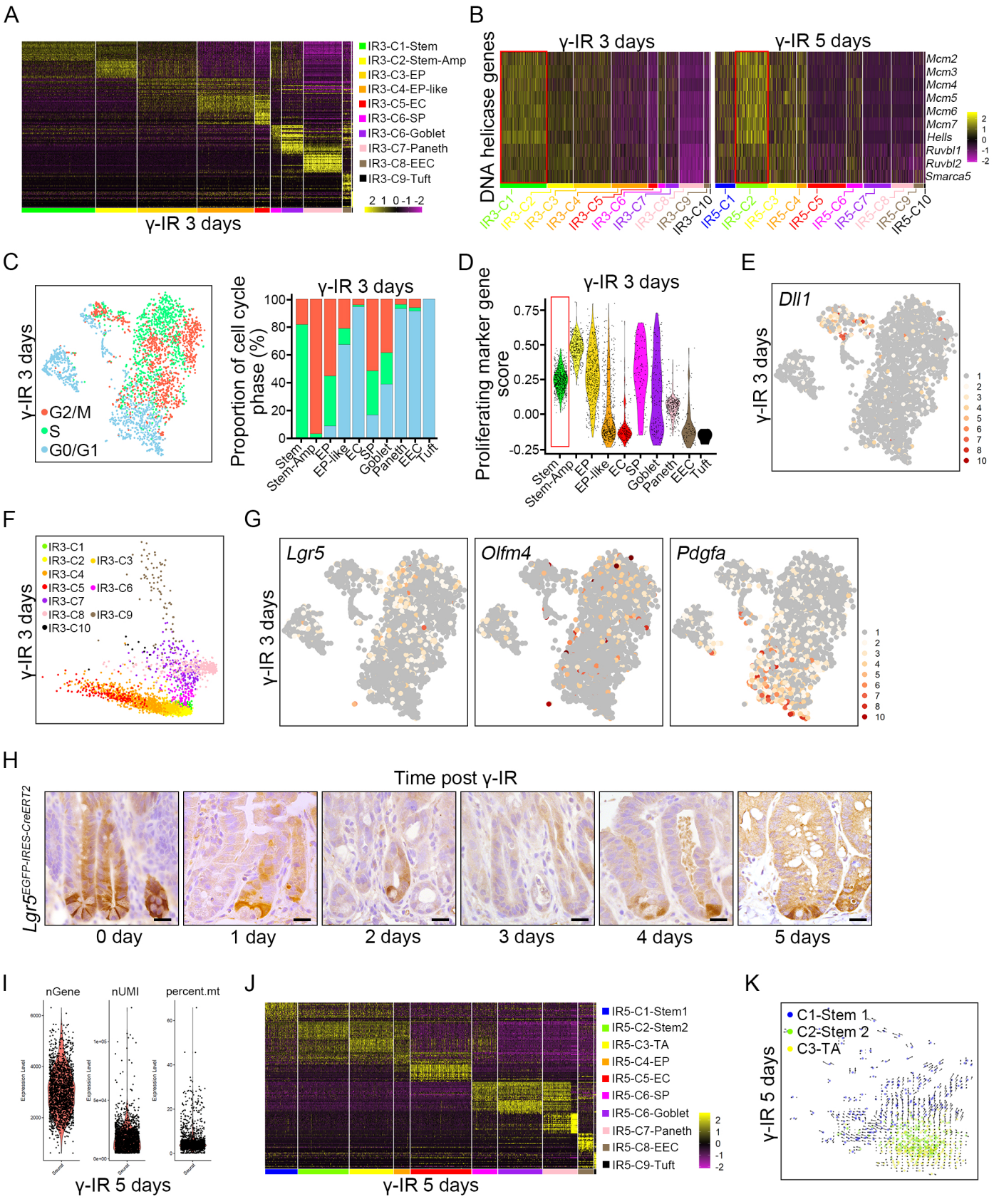

Figure S6. scRNA-seq analysis on *Msi1*$^{+}$ cell progeny three and five days after γ-IR. Related to Figure 5.

(A) Heatmap of differentially expressed genes in distinct clusters three days after γ-IR. (B) Heatmap of DNA helicase genes in distinct clusters at the indicated time points after γ-IR. (C) Cell cycle metrics of *Msi1*$^{+}$ cell progeny three days after γ-IR. t-SNE plot of the assigned cell cycle stages on *Msi1*$^{+}$ cell progeny. Proportion of cell cycle stages in each cluster three days after γ-IR. Cells in S phase are colored green, those in G2/M phase are red, and those in G0/G1 phase are blue. (D) Violin plots of proliferating marker gene score three days after γ-IR. (E) Feature plots of expression distribution for secretory progenitor marker *Dll1*. Expression levels for each cell are color-coded. (F) PCA analysis showing the association among distinct clusters three days after γ-IR. (G) Feature plots of expression distribution for CBC marker genes. Expression levels for each cell are color-coded. (H) Immunohistochemistry for GFP in the intestine of *Lgr5*$^{EGFP\text{-}IRES\text{-}CreERT2}$ mice at the indicated time points after γ-IR. Scale bar: 20 μm. (I) scRNA-seq data quality control of *Msi1*$^{+}$ cell progeny from *Msi1*^{CreERT2}*;R26*^{mTmG} mice five days after γ-IR. The mice were pretreated with tamoxifen fifteen hours before irradiation. The number of UMIs, genes, and mitochondrial percentage contents detected per cell. (J) Heatmap of differentially expressed genes in distinct clusters five days after γ-IR. (K) RNA velocity analysis of IR5-C1 to IR5-C3 across the PCA plot five days after γ-IR.

Figure S7 (Related to Figure 6)

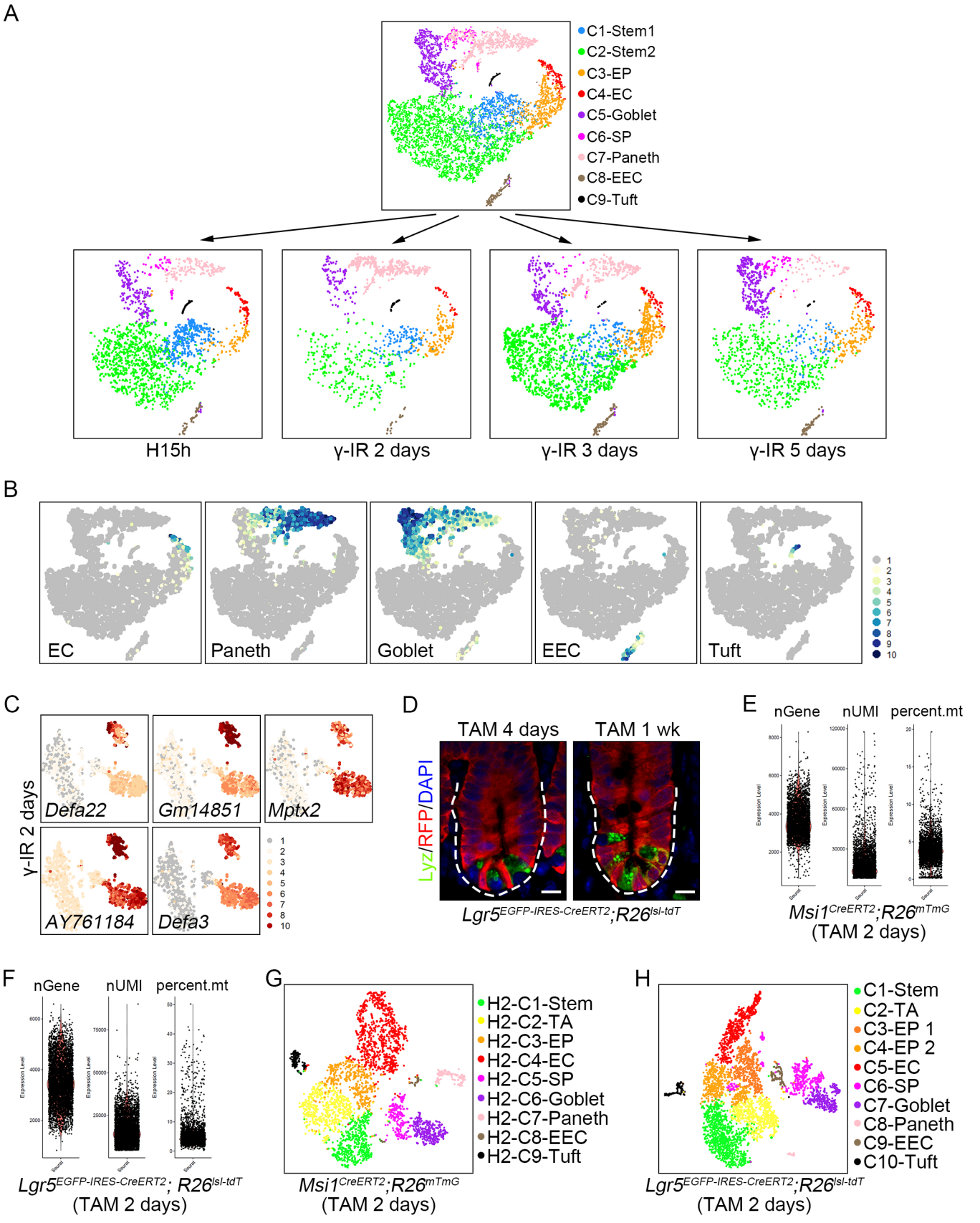

Figure S7. *Msi1*$^{+}$ cells preferentially generate Paneth cells. Related to Figure 6.

(A) A integrated t-SNE plot revealed cellular dynamic change of *Msi1*$^{+}$ cells progeny from *Msi1*^{CreERT2}*;R26*^{mTmG} mice at homeostasis, two, three and five days after γ-IR (Top). The mice were pretreated with TAM fifteen hours before γ-IR. The t-SNE plots showed the epithelium cell subtypes in individual samples (Bottom). (B) Mean expression ($\log_2$(TMP+1)) of several marker genes for a particular cell type shown on integrated t-SNE plots. The selected marker genes are identical to those in Figure S3B. (C) Feature plots of expression distribution for Paneth cell marker genes two days after γ-IR. Expression levels for each cell are color-coded. (D) Immunofluorescence for lysozyme and RFP in intestinal crypts from *Lgr5*$^{EGFP\text{-}IRES\text{--}CreERT2}$*;R26*$^{lsl\text{-}tdT}$ mice four and seven days after TAM induction. n=3 mice per chase timepoint. Scale bar: 10 μm. (E) scRNA-seq data quality control of *Msi1*$^{+}$ cell progeny from *Msi1*^{CreERT2}*;R26*^{mTmG} mice two days after tamoxifen induction. The number of UMIs, genes, and mitochondrial percentage contents detected per cell. (F) scRNA-seq data quality control of *Lgr5*$^{+}$ cell progeny from *Lgr5*$^{EGFP\text{-}IRES\text{--}CreERT2}$*;R26*$^{lsl\text{-}tdT}$ mice two days after TAM induction. The number of UMIs, genes, and mitochondrial percentage contents detected per cell. (G) A t-SNE plot reveals cellular heterogeneity, with nine distinct clusters of 3570 *Msi1*$^{+}$ cell progeny from *Msi1*^{CreERT2}*;R26*^{mTmG} mice two days after TAM induction. (H) A t-SNE plot revealed cellular heterogeneity with ten distinct clusters of 4555 *Lgr5*$^{+}$ cell progeny from *Lgr5*$^{EGFP\text{-}IRES\text{--}CreERT2}$*;R26*$^{lsl\text{-}tdT}$ mice two days after TAM induction.